Geo-Environmental Characterization of Coal Mine Waste Rock: Assessing its Potential to Generate Acid Mine Drainage

Ayoub El Aallaoui[1,*], Mustapha El Ghorfi[1,2], Abdellatif Elghali[2], Yassine Taha[2], Mostafa Benzaazoua[2] and Rachid Hakkou[2,3]

[1] *Laboratory of Geo resources, Geo environment and civil engineering, Faculty of Science and Technology Gueliz, Cadi Ayyad University, Avenue A. Elkhattabi, BP549, 40000 Marrakech, Morocco*

[2] *Geology sustainable mining laboratory institute (GSMI), Mohamed 6 polytechnic university (UM6P), Benguerir, Morocco*

[3] *Materials and Environmental Chemistry Laboratory (IMED-Lab), Faculty of Science and Technology Gueliz, Cadi Ayyad University, Avenue A. Elkhattabi, BP549, 40000 Marrakech, Morocco*

**ayoub.elaallaoui@ced.uca.ma*

Abstract

Coal mining generates coal mine waste rock (CMWR), which can pose environmental risks like acid mine drainage (AMD), contaminated neutral drainage (CND), or saline drainage, depending on pH and metal(loids) concentration. The Jerada T08 CMWR pile, deposited over 50 years ago, exemplifies this issue. To assess its environmental impact, a geo-environmental characterization was conducted, leading to a 3D model that highlights zones prone to acidity. Results identified 3.8 Mt of potentially acid-forming (PAF) materials, distributed heterogeneously mainly in highly oxidized upper zones. This approach enhances management strategies and reduces costs by enabling targeted mitigation and minimizing remediation efforts.

Keywords: Coal Mine Waste Rock, Acid Mine Drainage, Geochemistry, Environment, 3D modeling

Introduction

Mining provides significant economic benefits through the extraction of valuable elements, but it also generates substantial amounts of waste, leading to critical environmental challenges (Worlanyo and Jiangfeng 2021). Mining waste is broadly categorized into two types: waste rock (WR) and tailings. WR, produced during mineral extraction, is typically deposited in large piles with a wide particle size distribution. Although it is generally physically stable, it often lacks chemical stability (Amos *et al.* 2015; Elghali *et al.* 2019). Tailings, on the other hand, are fine-grained residues from flotation processes, usually deposited in slurries in impoundments. Wet tailings stored behind dams can exhibit low mechanical stability, and many tailings dam failures around the world have resulted in extensive environmental damage; tailings can also have low chemical stability (Aubertin *et al.* 2002; Lindsay *et al.* 2015). Coal mine waste rock (CMWR) from coal mining frequently contains iron sulfide minerals, which present significant environmental hazards due to their potential to generate acid mine drainage (AMD) (Nordstrom *et al.* 2015). AMD, a major mining environmental issue, occurs when sulfide minerals (primarily pyrite) are exposed to air and water in the absence of sufficient neutralizing minerals (Evangelou and Zhang 1995; Dold 2017). This process produces sulfuric acid and releases various contaminants, such as iron, copper, zinc, arsenic, and cadmium, into the environment. AMD is characterized by an acidic pH (below 4), which enhances the solubility of metals and facilitates their mobility (Nordstrom *et al.* 2015). Once initiated, it can persist for decades or even centuries after mine closure, posing a long-term threat to water resources (Bouzahzah *et al.* 2014).

Mitigating environmental concerns related to AMD in CMWR requires a thorough characterization of their physical, chemical, and mineralogical properties. Key physical parameters, such as particle size distribution (PSD), density, porosity, and specific surface area (SSA), are critical for understanding reactivity and AMD generation potential (Elghali *et al.* 2019, 2023). Chemical analyses, focusing on sulfur content and trace element concentrations, are essential for assessing leaching risks and acid production potential, which are crucial for predicting AMD formation and designing targeted remediation strategies (Escobar *et al.* 2021; El Aallaoui *et al.* 2024b). Mineralogical evaluations play a pivotal role in identifying sulfide minerals, the identification of oxidized zones, the presence of neutralizing minerals that buffer acidity, and the degree of sulfide liberation (Parbhakar-Fox *et al.* 2013; El Aallaoui *et al.* 2024a). Additionally, geochemical assessments using static and kinetic tests provide insights into the acid generation potential of CMWR and help pinpoint potentially acid-forming (PAF) zones (Benzaazoua *et al.* 2017; Tabelin *et al.* 2020). Mapping the distribution of PAF zones through 3D modeling enables the identification of highly reactive areas and enhances understanding of the factors influencing AMD rates and extent, offering a more effective approach to managing environmental risks (Blannin *et al.* 2023; El Aallaoui *et al.* 2024b). However, heterogeneity, limited understanding of oxidation pathways, and insufficient field data further hinder predictive accuracy of the models (Dold 2014; Simate and Ndlovu 2014). Addressing these gaps requires advanced modeling techniques, long-term field and laboratory studies to enhance AMD prediction.

This study introduces a novel approach for the Jerada province, focusing on the abandoned Jerada coal mine (closed since 2000) and its oldest waste pile (T08), deposited over 50 years ago (Fig. 1A). It offers a cost-effective strategy for managing CMWR by integrating environmental protection with sustainability. A baseline for PAF distribution and AMD risk was established through detailed chemical, mineralogical, and environmental analyses. Drone imagery provided topographic data and enabled PAF volume estimation (Fig. 1B), while 3D modeling uncovered spatial variations in acid generation potential (AGP), identifying previously unrecognized PAF zones within

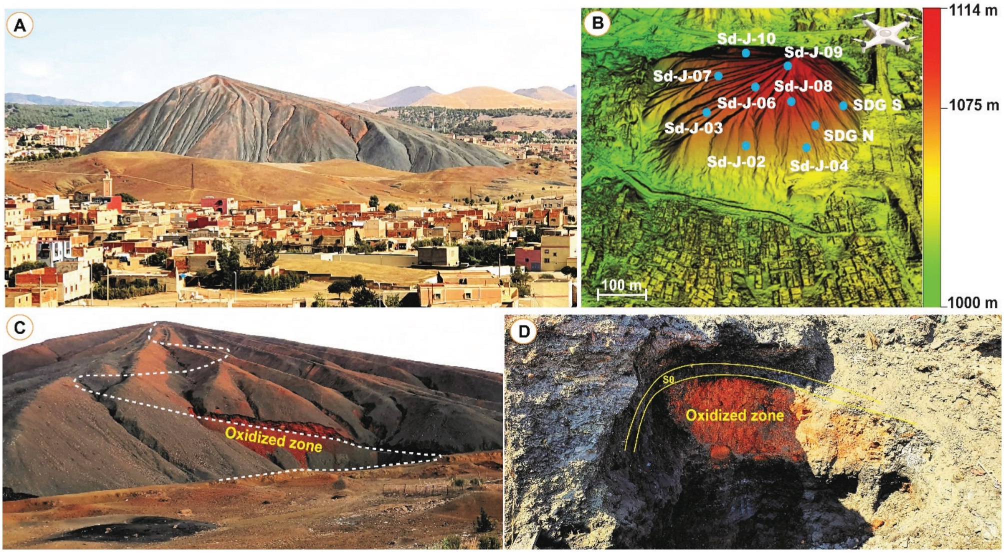

Figure 1 *Real image of the T08 CMWR pile; B: Topo-photogrammetric survey of T08 conducted via drone, highlighting the height of the pile and location of selected drillholes; C and D: On-site images of T08 showcasing the effects of oxidation.*

the CMWR pile. Samples from distinct oxidized zones (low and high oxidation) were analyzed for physical, chemical, and mineralogical characteristics using acid-base accounting (ABA) and net acid generation (NAG) tests to assess their environmental behavior (Fig. 1C, D).

Materials and Methods

The Jerada basin in eastern Morocco faces environmental and socio-economic challenges due to ten unrehabilitated CMWR piles, T01 to T10 (Jerada Archives 1990). T08, the largest, contains around 7.3 Mt of CMWR (Aallaoui *et al*. 2024; El Aallaoui *et al*. 2025) and reaches 100 m in height. Despite arid conditions, AMD remains a concern. A drone survey of 120 ha enabled precise topographic mapping and volume estimation of T08. Reverse circulation drilling retrieved 432 samples (~20 kg/m) (Tab. 1) that were dried, crushed to 100 µm, and analyzed to assess the potential environmental behavior of the pile. Two composite samples represented distinct oxidation zones. The low-oxidized sample (Sd-J-02, Sd-J-03, Sd-J-10, SDG N) exhibited black coal characteristics with relatively low pyrite and iron oxide content. Conversely, highly oxidized sample (SDG R, SDG A, Sd-J-06, Sd-J-08) showed more iron oxides content and reddish color, suggesting advanced oxidation. Analyses covered physicochemical, mineralogical, and environmental aspects. Particle size distribution was determined via wet sieving (for particles between 50 µm and 2 mm) and laser diffraction (for <500 µm). SSA was measured using the BET method. Major elements (SiO_2, Al_2O_3, TiO_2, Fe_2O_3, CaO, MgO, MnO, Na_2O, K_2O) were analyzed via XRF-EDS. Total carbon and sulfur were quantified using an induction furnace. Sulfates were measured via acid digestion (HCl) and spectrophotometry (at 650 nm). Trace elements were analyzed using ICP-MS following HNO_3-$HClO_4$ digestion, followed by controlled evaporation and dilution (1:8000) to prevent ICP-MS oversaturation. The AGP was assessed using static test (ABA) and NAG test. The NAG test, performed with H_2O_2 digestion, measured pH and electrical conductivity (EC) to further predict acid generation. Using 3D modeling, AGP zones were identified, correlating with oxidation areas to improve waste management through early PAF detection, targeted mitigation, and cost reduction. Geochemical and environmental data from over 200 points were processed in Datamine Studio RM to interpolate parameters like S-sulfate, S-sulfide, acidification potential (AP), and net neutralizing potential (NNP). Variogram analysis determined data distribution, and ordinary kriging was used for interpolation between and among measurements. Results were presented as wireframes with 6 × 6 × 2 m blocks and sub-blocks for precision.

***Table 1** Drill hole locations, depths, and inclinations for the T08 waste pile.*

Pile	Holes ID	X (m)	Y (m)	Z (m)	Depth (m)	Inclination (°)
T08	SDG A	796814.47	416002.24	1036.10	18	0
	SDG B	796856.30	416025.38	1032.42	52	0
	SDG N	797067.95	415939.83	1036.92	26	0
	SDG R	796930.50	416020.16	1039.59	58	0
	SDG S	797049.19	415994.44	1030.00	46	0
	Sd-J-02	797000.00	415700.00	1043.90	10	90
	Sd-J-03	796900.00	415700.00	1049.45	20	90
	Sd-J-04	797100.00	415800.00	1031.01	2	90
	Sd-J-06	796900.00	415800.00	1084.50	50	90
	Sd-J-07	796800.00	415800.00	1034.26	8	90
	Sd-J-08	797000.00	415900.00	1089.50	60	90
	Sd-J-09	796900.00	415900.00	1103.31	74	90
	Sd-J-10	796800.00	415900.00	1037.47	8	90

Results and discussion

The physical assessment of the CMWR pile revealed slight differences in particle size distributions between low-oxidized and high-oxidized zones. In low-oxidized areas, the D90 (particle diameter at 90% passing) was 353.3 µm, compared to 409 µm in high-oxidized zones (Fig. 2A). Mineral grain sizes ranged from 6 to 32 µm, with pyrite grains slightly larger in low-oxidized zones (8–18 µm). Iron oxide grains, particularly hematite, ranged from 10 µm in high-oxidized zones to 33 µm in low-oxidized areas (Fig. 2B). Finer pyrite particles in highly oxidized zones increased surface area, accelerating pyrite oxidation, though secondary iron oxide coatings often slowed further reactions, creating redox disequilibrium (Cravotta 1994; Evangelou and Zhang 1995). Chemical analysis revealed up to 13 wt.% carbon, with total sulfur ranging from 0.5–2 wt%, highest in SDG A, SDG B, and SDG R. Sulfate content varied from 0.12–16 wt%, peaking in SDG A, SDG B, and Sd-J-06, with concentrations decreasing with depth. ICP-MS analysis detected Cu (41 mg/L), Zn (122 mg/L), Pb (93 mg/L), Fe (66,556 mg/L), Ni (54 mg/L), Co (25 mg/L), and As (49 mg/L), while Cd and Ti were below detection limits. These trace element levels raise concerns about metal leaching during and after rainfall events. While previous toxicity leaching characteristic procedure (TCLP) studies (Taha *et al.* 2018) indicated that concentrations generally fall below hazardous leaching thresholds, long-term monitoring remains essential.

Mineralogical analysis highlighted the dominance of silicates minerals, with quartz constituting 37.1–38.3 wt% and clay minerals accounting for 31.7–33.1 wt%. Mica content ranged from 14.2 to 16.2 wt%, while plagioclase and chlorite were present in smaller percentages (4.92–5.34 wt% and 1.25–2.32 wt%, respectively). Calcite content varied from 2.32 wt% in low-oxidized zones to 3.55 wt% in high-oxidized zones. Iron oxides, such as hematite (1.53–1.8 wt.%) and goethite (2.17–3.2 wt.%), were more abundant in high-oxidized zones (Fig. 3A, B). QEMSCAN imagery provided further insights, highlighting a significant presence of iron oxides (Hematite and goethite). Traces of pyrite grains were observed in both low and high-oxidized zones, closely associated with surrounding gangue minerals (Fig. 3C, D). Furthermore, the limited presence of neutralizing minerals, such as carbonates, in these CMWR reduces the capacity to buffer acidity, increasing the vulnerability to acid generation.

The ABA results showed AP values of 14–41 kg $CaCO_3$/t, with lower levels (14–17 kg $CaCO_3$/t) in low-oxidized zones. NP was limited, and NNP ranged from −35 to −12 kg $CaCO_3$/t, classifying most samples as uncertain ($-20 < NNP < 20$), except SDG A, SDG B, SDG R, and Sd-J-09 (PAF, $NNP < -20$) (Fig. 4B). The neutralization potential ratio (NPR) varied from 0.16 to 0.36, confirming all samples as PAF ($NPR < 1$). NAG pH values ranged between 2.4 and 6.1, with solution acidity values of 4.32–42.5 kg H_2SO_4/t, exceeding standard limits. NPR plotted against

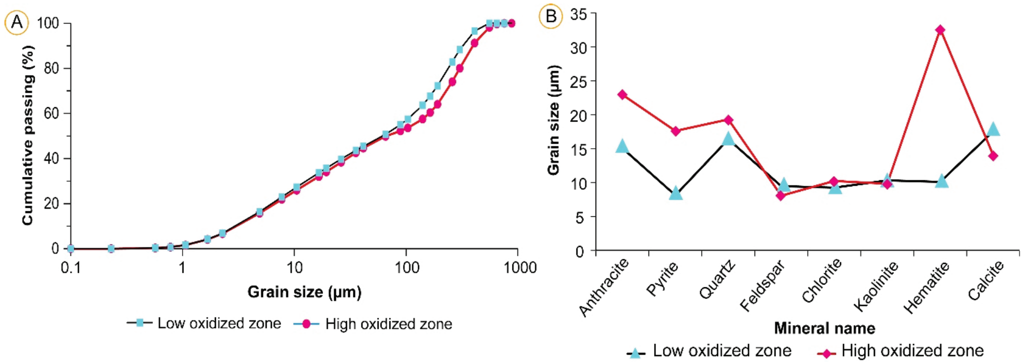

Figure 2 *A: Particle size distribution for low and high oxidized zones, B: Minerals grain size distribution for low and high oxidized zones.*

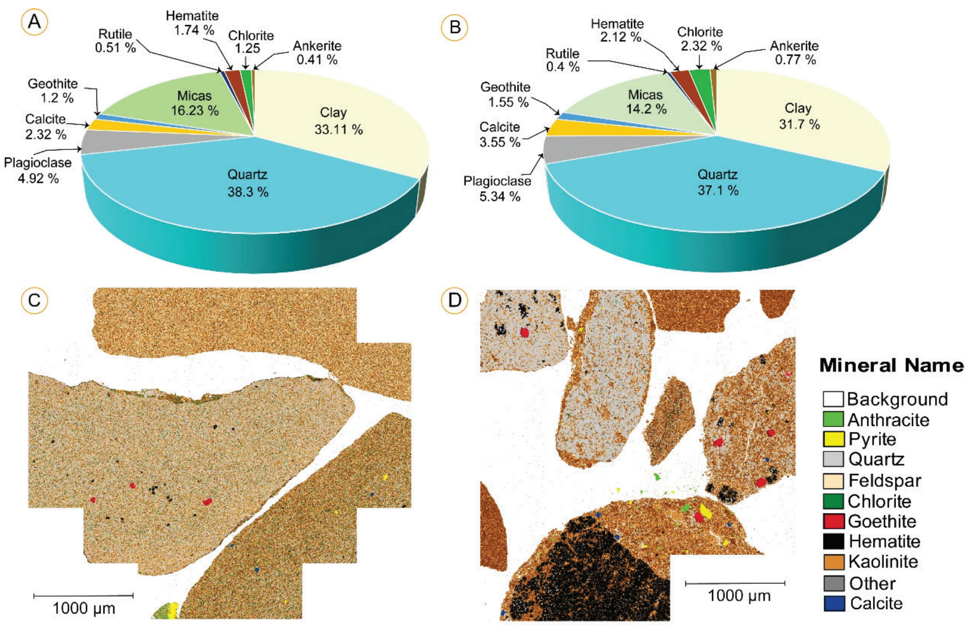

Figure 3 Mineralogical phases identified using QEMSCAN for A: low-oxidized and B: high-oxidized zones; QEMSCAN imagery for C: low oxidized and D: high oxidized zones.

NAG pH in Fig. 4A, showed most samples between uncertain classification (UC) and PAF, with NPR ranging from 1.61 to 79.33 and SDG R, Sd-J-06 exhibiting the highest AGP. EC varied from 0.12 to 1.28 µS/cm, peaking in SDG R, SDG A, and Sd-J-06. Jerada's CMWR exhibits predominantly AGP properties, with some areas falling within UC range. Therefore, long-term kinetic tests are crucial for further understanding of environmental behavior over time. A 3D geochemical block model was developed using 3D photogrammetric imagery and chemical analysis of drilled samples to map the spatial distribution of S-sulfate, S-sulfide, AP, and NNP. The model identified high S-sulfide content areas, indicating significant AMD potential. Ordinary kriging was used to interpolate these parameters, assuming a density of 1.60 kg/m^3. Results showed low S-sulfate contents in the core (<0.034 wt%) and higher near the surface due to oxidation. Total S-sulfide was estimated at 6.01 Mt (0.48 wt% average), with approximately 3.8 Mt of PAF material concentrated in the upper sections, while the remaining (approximately 3.5 Mt) were classified as uncertain (Fig. 4C, D).

Conclusion

This study pioneered the use of 3D mapping and modeling to identify PAF zones in the Jerada CMWR pile (T08). By integrating physical, chemical, and mineralogical data with high-resolution drone imagery, it mapped approximately 3.8 Mt of PAF material, mainly in the upper zones where high oxidation has increased sulfate content and AP. These findings enable targeted mitigation strategies to minimize long-term environmental and financial impacts.

Acknowledgements

This research was financially supported by the International Research Chairs Initiative, sponsored by Canada's International Development Research Centre (IDRC) and coordinated through the Canadian Research Chairs Program under Grant Numbers 108469-001 and 109418-006.

References

Aallaoui AE, El Ghorfi M, Elghali A, *et al* (2024) 3D Modeling and Resources Estimation of Coal Old Piles in Jerada Mine, Oriental Morocco. In: Çiner, A., *et al.* Recent Research on Sedimentology, Stratigraphy, Paleontology, Geochemistry, Volcanology, Tectonics,

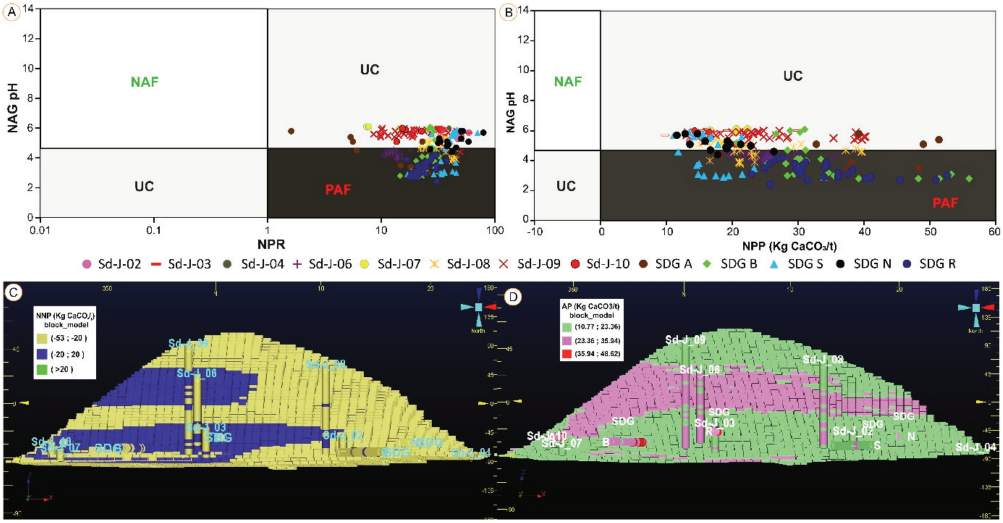

Figure 4 AMD prediction results for the T08 CMWR pile: (A) NPR vs. NAG pH, (B) NPP vs. NAG pH, (C) estimated block model of NNP (kg CaCO3/t), and (D) estimated block model of AP (kg CaCO3/t). NAF = non-acid forming, UC = uncertain classification, PAF = potentially acid forming.

and Petroleum Geology. MedGU 2022. Advances in Science, Technology & Innovation. Springer, Cham.

Amos RT, Blowes DW, Bailey BL, *et al* (2015) Waste-rock hydrogeology and geochemistry. Appl Geochemistry 57:140–156. https://doi.org/10.1016/j.apgeochem.2014.06.020

Aubertin M, Bussière B, Bernier L, *et al* (2002) La gestion des rejets miniers dans un contexte de développement durable et de protection de l'environnement. Congrès Annu la Société Can génie Civ GE-045:1–10

Benzaazoua M, Bouzahzah H, Taha Y, *et al* (2017) Integrated environmental management of pyrrhotite tailings at Raglan Mine : Part 1 challenges of desulphurization process and reactivity prediction. J Clean Prod 162:86–95. https://doi.org/10.1016/j.jclepro.2017.05.161

Blannin R, Frenzel M, Tolosana-Delgado R, *et al* (2023) 3D geostatistical modelling of a tailings storage facility: Resource potential and environmental implications. Ore Geol Rev 154:105337. https://doi.org/10.1016/j.oregeorev.2023.105337

Bouzahzah H, Benzaazoua M, Bussiere B, Plante B (2014) Prediction of Acid Mine Drainage: Importance of Mineralogy and the Test Protocols for Static and Kinetic Tests. Mine Water Environ 33:54–65. https://doi.org/10.1007/s10230-013-0249-1

Cravotta CA (1994) Secondary iron-sulphate minerais as sources of sulphate and acidity. In: Environmental Geochemistry of Sulfide oxidation

Dold B (2017) Acid rock drainage prediction: A critical review. J Geochemical Explor 172:120–132. https://doi.org/10.1016/j.gexplo.2016.09.014

Dold B (2014) Evolution of acid mine drainage formation in sulphidic mine tailings. Minerals 4:621–641. https://doi.org/10.3390/min4030621

El Aallaoui A, El Ghorfi M, Elghali A, *et al* (2024a) Investigating the reprocessing potential of abandoned zinc-lead tailings ponds : A comprehensive study using physicochemical , mineralogical , and 3D geometallurgical assessments. Miner Eng 209:108634. https://doi.org/10.1016/j.mineng.2024.108634

El Aallaoui A, El Ghorfi M, Hakkou R, *et al* (2024b) Integrated 3D geo-environmental assessment of acid-forming materials in historic coal waste piles for sustainable management. Chemosphere 370:143947. https://doi.org/10.1016/j.chemosphere.2024.143947

El Aallaoui A, Elghali A, Hakkou R, *et al* (2025) 3D geometallurgical characterization of coal mine waste rock piles for their reprocessing purpose. Int J Coal Sci Technol 12:. https://doi.org/10.1007/s40789-025-00756-7

Elghali A, Benzaazoua M, Bussière B, Bouzahzah H (2019) Determination of the available acid-generating potential of waste rock, part II: Waste management involvement. Appl. Geochemistry 100:316–325

Elghali A, Benzaazoua M, Taha Y, *et al* (2023) Prediction of acid mine drainage: Where we are. Earth-Science Rev 241:104421. https://doi.org/10.1016/j.earscirev.2023.104421

Escobar GA, Jorge E, Álvaro MRSR, Mafalda MMP (2021) Physical – Chemical Characterization of the Neves Corvo Extractive Mine Residues : A Perspective Towards Future Mining and Reprocessing of Sulfidic Tailings. J Sustain Metall 7:1483–1505. https://doi.org/10.1007/s40831-021-00428-1

Evangelou VP, Zhang YL (1995) A review: Pyrite oxidation mechanisms and acid mine drainage prevention A Review: Pyrite Oxidation Mechanisms and Acid Mine Drainage Prevention. Crit Rev Environ Sci Technol 25:37–41. https://doi.org/http://dx.doi.org/10.1080/10643389509388477

Jerada Archives (1990) Historique de la mine de Jerada. In: Charbonnages du Maroc (CDM) report – Exploitation et Enrichissement. pp 9–15

Lindsay MBJ, Moncur MC, Bain JG, *et al* (2015) Geochemical and mineralogical aspects of sulfide mine tailings. Appl Geochemistry 57:157–177. https://doi.org/10.1016/j.apgeochem.2015.01.009

Nordstrom DK, Blowes DW, Ptacek CJ (2015) Hydrogeochemistry and microbiology of mine drainage: An update. Appl Geochemistry 57:3–16. https://doi.org/10.1016/j.apgeochem.2015.02.008

Parbhakar-Fox A, Lottermoser B, Bradshaw D (2013) Evaluating waste rock mineralogy and microtexture during kinetic testing for improved acid rock drainage prediction. Miner Eng 52:111–124. https://doi.org/10.1016/j.mineng.2013.04.022

Simate GS, Ndlovu S (2014) Acid mine drainage: Challenges and opportunities. J Environ Chem Eng 2:1785–1803. https://doi.org/10.1016/j.jece.2014.07.021

Tabelin CB, Corpuz RD, Igarashi T, *et al* (2020) Acid mine drainage formation and arsenic mobility under strongly acidic conditions: Importance of soluble phases, iron oxyhydroxides/oxides and nature of oxidation layer on pyrite. J Hazard Mater 399:122844. https://doi.org/10.1016/j.jhazmat.2020.122844

Taha Y, Benzaazoua M, Edahbi M, *et al* (2018) Leaching and geochemical behavior of fired bricks containing coal wastes. J Environ Manage 209:227–235. https://doi.org/10.1016/j.jenvman.2017.12.060

Worlanyo AS, Jiangfeng L (2021) Evaluating the environmental and economic impact of mining for post-mined land restoration and land-use: A review. J Environ Manage 279:111623. https://doi.org/10.1016/j.jenvman.2020.111623